AIChE

PROCESS SYSTEMS ENGINEERING

Between-Phase-Based Statistical Analysis and Modeling for Transition Monitoring in Multiphase Batch Processes

Chunhui Zhao
Dept. of Chemical Engineering, University of California, Santa Barbara, CA 93106

Furong Gao
Dept. of Chemical and Biomolecular Engineering, The Hong Kong University of Science and Technology, Kowloon, Hong Kong SAR

DOI 10.1002/aic.12783
Published online October 18, 2011 in Wiley Online Library (wileyonlinelibrary.com).

Between-phase transition analysis and monitoring are a critical problem in multiphase (MP) batch processes. An improved statistical analysis, modeling, and monitoring strategy are proposed for MP processes with between-phase transition. It is realized that between-phase transition may show complex "irregular dynamics" over different batches. That is, transition patterns may follow different trajectories with different durations and reveal different characteristics in different batch cycles. Phase centers are defined to capture the transition irregularity, and the relationship between two neighboring phase centers is analyzed by performing between-phase analysis. Two different subspaces are thus separated in each phase, driven by the phase-common and dependent correlations, respectively. The basic assumption is that despite their different operation patterns, the two neighboring phases share a certain common correlations immune to phase shift. Then, reconstruction-based transition identification algorithm is designed, by which, between-phase transition can be supervised automatically and dynamically without the need of transition model development. The proposed method captures the between-phase transition from a new viewpoint. Its feasibility and performance are illustrated with a practical case. © 2011 American Institute of Chemical Engineers *AIChE J,* 58: 2682–2696, 2012

Keywords: multiphase batch process, between-phase analysis, irregular transition dynamics, phase-common and specific correlations, subspace separation, reconstruction-based transition identification

Introduction

Multivariate statistical techniques, such as multiway principal component analysis (PCA) and multiway partial least squares,[1–3] were introduced by Nomikos and Macgregor for batch process monitoring. Since then, many applications and extensions have been reported.[4–13] The subject of statistical modeling and monitoring arouses new issues and demand specific solutions when it refers to multiphase (MP) batch processes. Considering that the multiplicity of phases is an inherent nature of many batch processes and each phase exhibits different underlying behaviors, phase-based statistical analysis and monitoring strategies have been developed and achieved wide applications.[8,10,13–24] A batch process may be divided into several modeling phases as indicated by the changes of the inherent process correlation nature. Despite that the process may be externally time varying or nonstationary, the correlations of process variables are largely similar within the same phase, which can be characterized by a representative statistical model.[17] Multiple-phase models are thus developed for online monitoring. In this way, the behavior of each phase can be seen and, thus, more comprehensive process understanding can be expected. Here, it should be noted that as clearly stated in the previous work,[25] the divided phases, which more exactly, may be called as "modeling phases," are defined from the viewpoint of statistical meaning. They focus on reflecting the changes of the underlying correlation characteristics and may be different from the real physical "operating phases." For simplicity, they are uniformly called "phase" in this work unless otherwise noted. Yao and Gao[25] gave an overview of MP statistical analysis methods for process analysis, monitoring, quality prediction, and online quality improvement, where different types of phase division and phase-based modeling strategies in the previous literature were analyzed and discussed.

However, the conventional phase partition algorithms divided each sample into one definite phase and neglected the phase-to-phase transition characteristics. MP batch processes can operate in a variety of steady phases and between-phase dynamic transitions. Traditional-phase models experience a mismatch problem during transition regions as transition patterns may compromise the accuracy of phase representative models. Thus, the monitoring performance may be jeopardized, and frequent false alarms may be caused even though the process is actually under normal status. Considering the phase transition phenomena are common in industry batch processes, it is significant and promising to investigate the

Correspondence concerning this article should be addressed to F. Gao at kefgao@ust.hk.

transiting characteristics. As a challenging problem, the real-time monitoring of phase transition has drawn increasing attention recently. Up to now, there are only two works reported to solve the phase transition problem. Zhao et al.[26] first proposed the idea of phase transition monitoring and developed a soft transition multiple PCA modeling algorithm. The hard *k*-mean clustering algorithm was modified by defining two radiuses and ambiguous phase boundary. The transition regions between two neighboring phases were separated and given fuzzy memberships based on their relationships with the two-phase models. However, the membership grade, which evaluated the similarity of transition pattern to the phase behavior, was calculated based on Euclidean distance between the time-slice PCA loadings and phase PCA loadings. Its accuracy might influence the transition model. Moreover, the size of transition regions depended on the subjective choice of two radiuses. Yao and Gao[27] calculated the angles between different PCA models to identify the transition automatically without user-specified parameters. The membership parameters in transition models were calculated by solving an optimization problem to maximize the similarities between the transition time-slices and the neighboring phases.

Actually, the above methods both identify and fix the transition models *a priori* based on their relationships with two neighboring phases. The basic assumption is that each transition pattern follows fixed characteristics at certain between-phase time. Although they realize the dynamics of transition patterns along time direction, the predefined transition models may not be enough to capture the complex transition behavior. It is common that the between-phase operation patterns show the gradual changeover between two neighboring phases and also yield local fluctuation. Regularly, at the beginning they have the underlying characteristic more similar to the starting phase, whereas at the end they behave more similar to the target one. This can be called as "time-varying dynamics" within the same batch cycle. However, uncertainty is also observed from batch to batch. That is, the transition may go through different between-phase transition trajectories, start earlier or later, and progress faster or slower. Therefore, even at the same given time, the transition pattern may reveal different characteristics from those in other batches considering the complex situation of unstable transition behaviors. This results in batch-wise "irregular" transition patterns. Here, it can be called as "batch-varying dynamics" in opposite to previously well-recognized time-varying dynamics. From this viewpoint, the transition pattern may not be characterized comprehensively by a fixed statistical model. On the other hand, previous work on MP and transition modeling methods isolated each individual phase and did not consider the between-phase interrelationship. In reality, despite the difference between two neighboring phases, they also share a certain similarity. The between-phase transition is actually mainly reflected by the changes of phase-specific characteristics as phase-common information stays invariable during the transition progress. Despite the importance of between-phase transition monitoring, the above problems have not been addressed yet.

In this work, between-phase analysis is performed for MP modeling and online monitoring. Especially, focusing on between-phase transition behaviors, the batch-wise "irregularity" is analyzed, and transition behavior is comprehended and tracked from a novel viewpoint. Instead of adopting isolated phase modeling, it is necessary to first gain a detailed insight into the underlying characteristics of two neighboring phases, which can provide important information for transition analysis. It is found that despite the switch between phases, it does not mean that all underlying correlations change to completely different ones. It is easy to understand that some of the underlying correlation information remains the same and are consistent over two neighboring phases, which can be well approximated by a uniform statistical model. And more similarity should be observed between two neighboring phases than those nonadjacent ones. Other underlying information changes from phase to phase, revealing the between-phase difference in their underlying characteristics. It is clear that the phases are actually distinguished by this part of information. Motivated by such a finding, a two-step multiset variable correlation analysis (MsVCA),[28] which was proposed to relate the inherent variable correlations over multiple data spaces, can be used here as the basic modeling method. Following the development of a theoretical algorithm along with its property analysis in the previous work,[28] this study addresses the potential of using the aforementioned algorithm to solve the between-phase transition problem. With this method, the original phase measurement space can be separated into two different subspaces, where each subspace contains different underlying information. One subspace is called the common subspace that is spanned within each phase by the common bases. The other is called the noncommon subspace that is supported by those specific bases in each phase. Correspondingly, the underlying characteristics of each phase are separated, with the common and noncommon subspaces accounting for the between-phase similarity and dissimilarity, respectively. The separation of the common and specific information among different phases and the attention given to both provide a good platform for transition analysis. Only steady-phase models are built with corresponding monitoring confidence interval. No fixed monitoring systems are needed in advance for any between-phase transitions considering the "batch-wise irregularity." This is quite different from the previous work,[26,27] where the membership grades were calculated to get transition models beforehand. During online application, the transition behaviors can be supervised dynamically by checking whether it can be well described by the associated neighboring-phase models. It is based on the basic assumption that although the transition behaviors at some time show batch-to-batch oscillation, the underlying characteristics show the changes from the starting phase toward the target phase.

The rest of this article is organized as follows. First, the between-phase transition problem is stated for MP batch processes. The MsVCA algorithm[28] is revisited, and its feasibility for between-phase analysis is also revealed. Subsequently, the proposed between-phase modeling and monitoring procedure are formulated in detail. The underlying principle support is described, and its suitability and rationality are highlighted. In the following section, the application to a practical case is illustrated, in which, the presented recognition and argument are verified by the results. Finally, conclusions are drawn in the last section.

Methodology

Between-phase transition analysis

In MP batch processes, between-phase changeovers are frequent. Commonly, the process actually covers steady status and dynamic transition status from its previous phase or

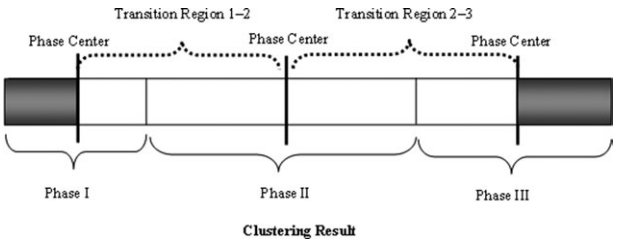

Figure 1. Illustration of between-phase analysis based on a simple three-phase process.

to its next phase. The questions of whether the process conditions during transitions are correct and how to assess the successful completion of a transition are attracting increasing attention,[26,27] yet still having challenges not met up to now. Valid process monitoring during transitions is important to guarantee stable and good transition performance. Commonly, the transition pattern shows the gradual changes starting from the first phase and toward the second phase and stays in a steady status after reaching the second phase. Then, at the end of the second phase, the process will go through another transition from the current phase toward the third one. The underlying characteristics of the transition patterns at the beginning resemble the characteristics of the start phase, whereas those later in the transition resemble the characteristics of the target steady phase. That is, the transition pattern can be interpreted with models of start phase and target phase. When a large number of process measurements are collected, one could make use of data-based multivariate statistical analysis methods to predefine the transition region in a lower feature subspace to ensure that the new transitions follow an acceptable path. However, resulting from the complexity of between-phase transition behavior, such as varied trajectories, duration, and starting time, the underlying transition characteristics are also irregular over batches. It is hard to distinguish the clear boundary between the steady phase and transition. Thus, it is impossible to characterize all possible transition patterns closely enough by fixed statistical models. Moreover, those transition patterns may not show consistent between-phase evolving trend. Sometimes, reversion is noticed, where the later transition may be more similar with the previous phase than those transition patterns before it. On the other hand, it is generally unfeasible that modeling samples are sufficient enough to cover all possible transition patterns. The new transition patterns that emerge during online application and show different characteristics against the reference ones may be detected as abnormal occurrence.

To accommodate the transition uncertainty, in our method, there is no need to fix the clear boundary between steady phase and transition regions from reference batches. Instead, phase centers, which are supposed to be in steady status, are defined by the sample in the middle time in each phase as shown in Figure 1, taking a simple three-phase process for instance. If there are even samples in this phase, the middle two can be used as the centers. In extreme case, the earliest transition may start right after the center of the starting phase and the latest one may end right before the center of the target phase. To more comprehensively accommodate all possible transition cases, the operation patterns between the centers of two adjacent phases are all regarded to be possible transitions. This is different from the previous method,[26,27] which first fixed the transition region and separated it from the steady phase region before modeling. Generally, the farther from the starting phase center and nearer to the target phase center, the more possible it is to be in transition status or even in the steady status of the target phase. For each phase (except the first and last phases), it can be separated by the phase center into two halves, the transition region from its previous phase and the transition region to its next phase. From the process beginning, for any operation pattern, based on the current time, there are three cases that should be considered based on the illustration in Figure 1:

1. if it is before Phase Center I (the gray area), it is regarded to be operating in steady status in Phase I as no phase is adjacent to this region;

2. if it is between the centers of Phases I and II, it is possible that it may be operating in steady status in Phase I or II or it may lie in between-phase transition from Phase I to Phase II. The scenario is the same for those samples between the centers of Phases II and III;

3. if it is after Phase Center III (the gray area), it is regarded to be operating in steady status in Phase III as no phase is adjacent to this part.

Based on the above analysis, the basic idea of the proposed method is as each transition pattern always shows different similarity with its neighboring phases, any normal transition pattern can be well accommodated by the two concerned phase models. This is the basic difference between a normal transition and abnormal process behavior. Moreover, instead of forcibly formulating a fixed transition model at each time, it is more desirable to dynamically describe each transition pattern by time-varying combinations of the two phases, where the ratio that each phase model plays is determined automatically by the current specific transition characteristics and its respective relationships with the two adjacent phases.

Moreover, from between-phase viewpoint, although one part of the underlying correlations changes from phase to phase, there is still one part of process correlations that stays invariable. Here, this is referred as "partial between-phase dissimilarity" as opposed to previous common recognition. The phase-common correlations are immune to the phase shift as they are similar in the two neighboring phases, whereas the phase-specific correlations change with the phase changeover. Clearly, it is the between-phase different correlations that distinguish the two adjacent phases, which can more clearly track the progressing of each transition pattern from starting phase to the target phase. So the key is how to separate the two different types of correlations in each phase. Therefore, the underlying information in each phase should be modeled in quite a different form from the conventional ones.

Motivated by such cognition, a two-step MsVCA[28] algorithm, which was proposed to relate the inherent variable correlations over multiple data spaces, can be used here as the basic modeling method. It should be noted that here only the between-set analysis is conducted as transition only happens between two neighboring phases. Following the development of a theoretical algorithm along with its property analysis in the previous work,[28] this study addresses the potential of using the aforementioned algorithm to solve the between-phase transition problem. For readability, a brief presentation of this algorithm is given in Appendix. By this algorithm, within each phase, the original measurement space can be separated into two different subspaces. One is called the common subspace, revealing the similar between-

phase underlying correlations. The other is called the specific subspace enclosing the different correlations between two adjacent phases. In comparison to the traditional statistical techniques, the separation of the common and specific correlations and the dual care paid to both are the major differences. In this way, one can better characterize and monitor the transition behavior by checking the phase-common and specific information, respectively.

Between-phase subspace separation

In each batch run, assume that J process variables are measured online at $k = 1, 2, \ldots, K$ time instances throughout the batch. Then, process observations collected from similar I batches can be organized as a three-way array $\underline{\mathbf{X}}$ ($I \times J \times K$). At each time, the means of each column are subtracted to approximately eliminate the main nonlinearity. And each variable is scaled to unit variance to handle different measurement units, thus giving each equal weight. In this work, the batches are of equal length without special declaration so that the specific process time can be used as an indicator for data normalization.

Phase information should be identified before between-phase analysis. In MP modeling, one important issue is how to get the phase marks (i.e., phase division) before designing the phase model. Various strategies[8,10,17–22] have been reported from different viewpoints and based on different principles, providing a rich database for phase division, and can be put into practical process monitoring. Besides the *a priori* mechanism knowledge-based phase partition methods,[8,10] several automatic phase division algorithms have been presented. Lu et al.[17] developed a k-mean clustering algorithm based on time-slice PCA loadings, which are supposed to reveal the underlying variables correlations. The consecutive similar PCA loadings will be collected in the same class (phase), and clustering result generally agrees well with the process time. Camacho and Pic proposed a MP algorithm[18,19] for automatic phase identification so that each segment of the batch can be well approximated by a linear PCA model with acceptable nonexplained variance. In this work, assuming that no prior process knowledge is available, C phases can be readily identified along time direction by clustering algorithm as what was done by Lu et al.[17] Certainly, the phase information can also be modified based on clustering result using prior expertise. Then the phase centers are obtained in each phase, which represent the steady phase status, $\mathbf{X}_i$ ($IN_i \times J$) ($i = 1, 2, \ldots, C$), where I is the number of batches and N_i is the number of time samples chosen as the phase centers. Generally, N_i is 1 and 2 corresponding to even and odd samples in each phase as mentioned before.

The between-phase similarity is deemed to be driven by some common basis vectors. Using MsVCA algorithm, the common bases are extracted focusing on two adjacent phases, which are representative enough of the other samples and can substitute all samples by their linear combinations. They can be used as the key evaluation index of the between-phase similarity. Here, it should be noted that for each phase, when it is analyzed with different adjacent phases, the analysis result may be different. For example, regarding Phase 2, for transition regions 1 and 2 and for transition regions 2 and 3, respectively, the between-phase models are different. For C phases, there are $C - 1$ between-phase combinations that should be analyzed.

For any two adjacent phases, $\mathbf{X}_i$ ($IN_i \times J$) and $\mathbf{X}_{i+1}$ ($IN_{i+1} \times J$), which may have a different number of samples but the same variables, the between-phase common global bases are obtained by MsVCA: $\mathbf{P}_g$ ($J \times R^c$), where R^c is the retained number of common bases. Then each original observed data space ($\mathbf{X}_i$) is separated into two different parts, $\mathbf{X}_i{}^c$ and $\mathbf{X}_i{}^s$

$$\begin{aligned}
&\mathbf{X}_i = \mathbf{X}_i^c + \mathbf{X}_i^s \\
&\mathbf{X}_i^{cT} = \mathbf{P}_g\mathbf{B}_i^c = \mathbf{P}_g\left(\mathbf{P}_g^T\mathbf{P}_g\right)^{-1}\mathbf{P}_g^T\mathbf{X}_i^T = \mathbf{P}_g\mathbf{P}_g^T\mathbf{X}_i^T \\
&\mathbf{X}_i^{sT} = \mathbf{X}_i^T - \mathbf{X}_i^{cT} = \left(\mathbf{I} - \mathbf{P}_g\mathbf{P}_g^T\right)\mathbf{X}_i^T
\end{aligned} \tag{1}$$

where $\mathbf{B}_i^c = (\mathbf{P}_g^T\ \mathbf{P}_g)^{-1}\ \mathbf{P}_g^T\ \mathbf{X}_i^{cT}$ is the linear combination coefficient corresponding to the common bases. Actually, $\mathbf{G}_{\mathbf{P}_g} = \mathbf{P}_g\,(\mathbf{P}_g^T\,\mathbf{P}_g)^{-1}\,\mathbf{P}_g^T = \mathbf{P}_g\mathbf{P}_g^T$ is the orthogonal projector onto the column space of $\mathbf{P}_g$, and $\mathbf{H}_{\mathbf{P}_g} = \mathbf{I} - \mathbf{G}_{\mathbf{P}_g} = \mathbf{I} - \mathbf{P}_g\mathbf{P}_g^T$ is the antiprojector with respect to the column space of $\mathbf{P}_g$. Therefore, from another viewpoint, the two subspaces can also be regarded as the ones obtained by projecting $\mathbf{X}_i$ onto the projectors, $\mathbf{X}_i\mathbf{G}_{\mathbf{P}_g}$ and $\mathbf{X}_i\mathbf{H}_{\mathbf{P}_g}$. It is clear that the two subspaces are orthogonal to each other as $\mathbf{X}_i^c\,(\mathbf{X}_i^s)^T = \mathbf{X}_i\,\mathbf{G}_{\mathbf{P}_g}\,(\mathbf{X}_i\mathbf{H}_{\mathbf{P}_g})^T = 0$. By between-phase analysis, one can find more meaningful intrinsic information hidden in each phase.

Moreover, from Eq. 1, the linear combination coefficients or regression coefficients $\mathbf{B}_i^c$ ($R^c \times IN_i$) are actually calculated by projecting $\mathbf{X}_i^c$ directly onto the common bases

$$\mathbf{B}_i^c = \mathbf{P}_g^T\mathbf{X}_i^{cT} = \mathbf{P}_g^T\left(\mathbf{X}_i\mathbf{G}_{\mathbf{P}_g}\right)^T = \mathbf{P}_g^T\mathbf{P}_g\mathbf{P}_g^T\mathbf{X}_i^T = \left(\mathbf{X}_i\mathbf{P}_g\right)^T \tag{2}$$

However, it should be noted that these combination coefficients in the common subspace are not guaranteed to be orthogonal to each other.

In the phase-common subspace, the observations/objects enclose the same underlying correlations as all of them are the linear combinations of common bases, which can be used as the uniform statistical model common to two adjacent phases. Also it should be noted that the linear combinations in each neighboring phase may be different, representing different variances along common bases.

In the phase-specific subspace, the objects contain no information associated with the common bases and, thus, are different and specific to each phase, revealing their dissimilarity. Therefore, different model structures should be designed for each subspace. Moreover, these objects are not guaranteed to cover only the systematic information. The traditional PCA decomposition is performed in each specific subspace to separate the systematic information and the noise information

$$\begin{aligned}
&\mathbf{T}_i^s = \mathbf{X}_i^s\mathbf{P}_i^s = \mathbf{X}_i\left(\mathbf{I} - \mathbf{P}_g\mathbf{P}_g^T\right)\mathbf{P}_i^s \\
&\hat{\mathbf{X}}_i^s = \mathbf{T}_i^s\mathbf{P}_i^{sT} \\
&\mathbf{E}_i^s = \mathbf{X}_i^s - \hat{\mathbf{X}}_i^s
\end{aligned} \tag{3}$$

where $\mathbf{P}_i^x$ ($J \times R_i^s$), the specific PCA loadings in each phase, reveal the major variation directions specific to each phase and R_i^s is the retained PC number. $\mathbf{E}_i^s$ is the specific-to-phase residual, and it is also the final noise error. In this way, each specific-to-phase subspace is further divided into two parts: the systematic specific variation information and the final noise errors. Generally, $\mathbf{P}^s$ ($J \times R_i^s$) should be more different between phases if those common bases are all excluded.

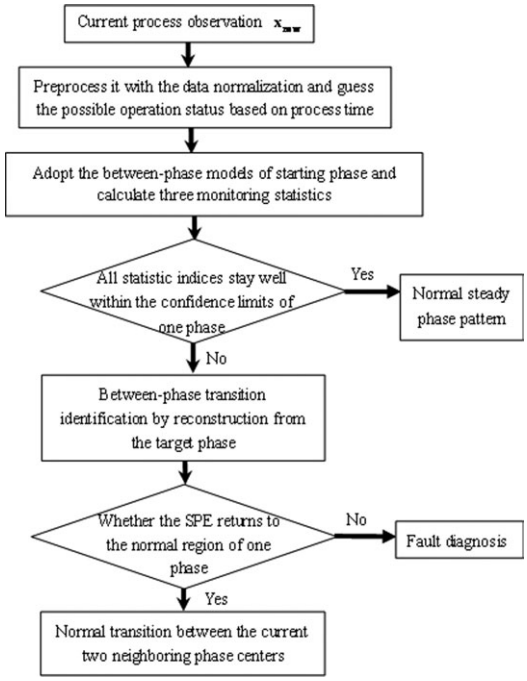

Figure 2. Flow chart of between-phase transition monitoring.

Moreover, it is clear that the specific bases are orthogonal to those common bases resulting from $\mathbf{X}_i^c$ $(\mathbf{X}_i^s)T = \mathbf{0}$. Therefore, the phase-specific scores $\mathbf{T}_i^s$ can also be obtained by directly projecting the original phase measurement ($\mathbf{X}_i$) onto $\mathbf{P}_i^s$: $\mathbf{T}_i^s = \mathbf{X}_i\,\mathbf{P}_i^s$.

From another viewpoint, as $\mathbf{P}_i^s = \mathbf{X}_i^{sT}\mathbf{T}_i^s(\mathbf{T}_i^{sT}\mathbf{T}_i^s)^{-1}$, these PCA loadings can also be expressed as one form of linear combination of the original measurement, and can thus be regarded as the basis vectors. Moreover, in the specific subspace, each sample in $\hat{\mathbf{X}}_i^s$ can be reconstructed by the linear combination of $\mathbf{P}_i^s$, in which, the combination coefficients are actually the orthogonal specific scores $\mathbf{T}_i^s$ ($IN_i \times R_i^s$).

In summary, the underlying characteristics of steady status covered by each phase center are formulated in two subspaces as follows

$$\begin{aligned}\mathbf{X}_i &= \mathbf{X}_i^c + \mathbf{X}_i^s \\ &= \mathbf{X}_i^c + \hat{\mathbf{X}}_i^{sT} + \mathbf{E}_i^s \\ &= \mathbf{X}_i\mathbf{P}_g\mathbf{P}_g^T + \mathbf{X}_i\mathbf{P}_i^s\mathbf{P}_i^{sT} + \mathbf{E}_i^s \\ &= \mathbf{B}_i^c\mathbf{P}_g^T + \mathbf{T}_i^s\mathbf{P}_i^{sT} + \mathbf{E}_i^s \\ &= \mathbf{X}_i\left(\mathbf{P}_g\mathbf{P}_g^T + \mathbf{P}_i^s\mathbf{P}_i^{sT}\right)^T + \mathbf{E}_i^s \\ &= \mathbf{X}_i\left[\mathbf{P}_g, \mathbf{P}_i^s\right]\left[\mathbf{P}_g, \mathbf{P}_i^s\right]^T + \mathbf{E}_i^s \\ &= \mathbf{X}_i\boldsymbol{\Omega}_i\boldsymbol{\Omega}_i^T + \mathbf{E}_i^s\end{aligned} \tag{4}$$

where for each phase, the complete systematic model, $\boldsymbol{\Omega}_i = [\mathbf{P}_g,\ \mathbf{P}_i^s]$, describes both common-to-phase and specific-to-phase systematic correlations. Correspondingly, $\mathbf{B}_i^c$ and $\mathbf{T}_i^s$ are their associated variations or their contributions.

Between-phase monitoring system

For different phase centers, from the between-phase viewpoint, different monitoring systems can be designed. Based on between-phase subspace separation result, two types of statistics are commonly calculated: the T^2-statistic that describes the systematic part captured by monitoring models and the Q-statistic that represents the residual part unoccupied by monitoring models. They are calculated as follows for each subspace

$$\begin{aligned}T_{i,k}^{c2} &= (\mathbf{b}_{i,k}^c - \bar{\mathbf{b}}_i^c)^T\mathbf{O}_{i,c}^{-1}(\mathbf{b}_{i,k}^c - \bar{\mathbf{b}}_i^c) \\ T_{i,k}^{s2} &= (\mathbf{t}_{i,k}^s - \bar{\mathbf{t}}_i^s)^T\mathbf{O}_{i,s}^{-1}(\mathbf{t}_{i,k}^s - \bar{\mathbf{t}}_i^s) \\ \mathrm{SPE}_{i,k}^s &= \mathbf{e}_{i,k}^{sT}\mathbf{e}_{i,k}^s\end{aligned} \tag{5}$$

where $\mathbf{b}_{i,k}^c$ ($R^c \times 1$) and $\mathbf{t}_{i,k}^s$ ($R^c \times 1$) are the common and specific score vectors of the observation at the kth sample time, respectively. $\bar{\mathbf{b}}_i^c$ and $\bar{\mathbf{t}}_i^s$ denote the corresponding mean vectors, both of which are zero vectors resulting from the mean centering during data preprocessing; $\mathbf{O}_{i,c}$ ($R^c \times R^c$) and $\mathbf{O}_{i,s}$ ($R_i^s \times R_i^s$) are the variance–covariance matrices of components, respectively. $\mathbf{e}_{i,k}^s$ ($J \times 1$) is the residual.

In each phase, the original measurement samples are deemed to follow a multivariate Gaussian distribution. Therefore, the linear combination coefficients corresponding to the bases should also follow this distribution. This premise provides an important basis for deriving the confidence limits of monitoring statistics. So the control limits in the systematic subspace for each phase are defined by the F-distribution with α as the significance factor[29,30]

$$T_i^2 \sim \frac{R(N_i^2 - 1)}{N_i(N_i - R)}F_{R,N_i-R,\alpha} \tag{6}$$

Similarly, in the residual subspace, the representative confidence limit of squared prediction error (SPE) for each

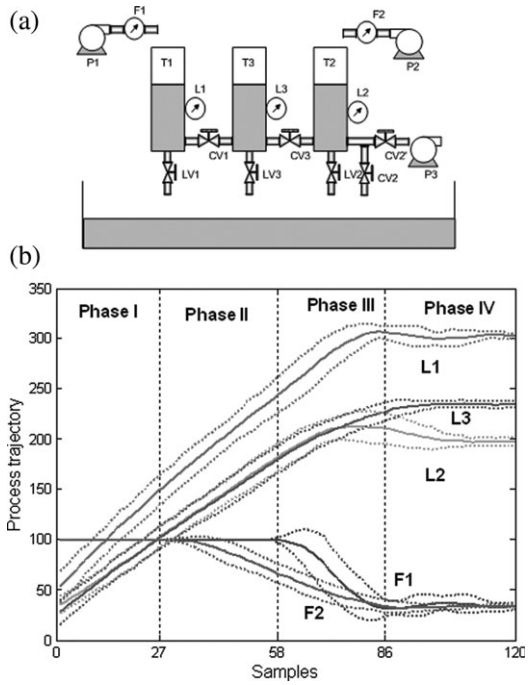

Figure 3. (a) Scheme of the three-tank system and (b) Mean process operation trajectories and the STD along with phase clustering information (I–IV) throughout one batch cycle.

Table 1. Between-Phase Analysis Results

Between-phase #		I	II	II	III	III	IV
Number of specific bases		1	1	1	2	1	2
$\mathbf{P}_g$		$\begin{bmatrix} 0 \\ -0.0000 \\ -0.9433 \\ 0.2975 \\ 0.1473 \end{bmatrix}$		$\begin{bmatrix} -0.0000 \\ -0.2229 \\ 0.1140 \\ 0.8295 \\ 0.4992 \end{bmatrix}$		$\begin{bmatrix} -0.3748 \\ -0.4923 \\ 0.3847 \\ 0.3275 \\ 0.6016 \end{bmatrix}$	
Variations	First $\mathbf{P}_g$ (%)	10.74	7.91	64.03	30.39	67.64	20.78
	First $\mathbf{P}_c^s$ (%)	86.50	85.01	29.70	52.82	24.62	52.88
	First $\mathbf{P}_g + \mathbf{P}_c^s$ (%)	97.24	92.92	93.73	83.21	92.26	73.66

phase can be approximated by a weighted Chi-squared distribution[2,31,32]

$$\mathrm{SPE}_i \sim g_i \chi^2_{h_i,\alpha} \tag{7}$$

where $g_i = v_i/2m_i$ and $h_i = 2(m_i)^2/v_i$, in which, m_i is the average of all the SPE values for the ith phase calculated in Eq. 6, and v_i is the corresponding variance.

Then the prepared monitoring systems are used for between-phase transition analysis and dynamic monitoring.

1. The patterns before the first phase center and after the last phase center are not in between-phase transition. They are directly projected on the corresponding phase center models

$$\begin{aligned}
\mathbf{b}^{\mathrm{c}}_{\mathrm{new}} &= \mathbf{P}_{\mathrm{g}}\mathbf{x}_{\mathrm{new}} \\
\mathbf{x}^{\mathrm{c}}_{\mathrm{new}} &= \mathbf{P}_{\mathrm{g}}\mathbf{b}^{\mathrm{c}}_{\mathrm{new}} = \mathbf{P}_{\mathrm{g}}\mathbf{P}_{\mathrm{g}}^{\mathrm{T}}\mathbf{x}_{\mathrm{new}} \\
\mathbf{x}^{\mathrm{s}}_{\mathrm{new}} &= \mathbf{x}_{\mathrm{new}} - \mathbf{x}^{\mathrm{c}}_{\mathrm{new}} = \left(\mathbf{I} - \mathbf{P}_{\mathrm{g}}\mathbf{P}_{\mathrm{g}}^{\mathrm{T}}\right)\mathbf{x}_{\mathrm{new}} \\
\mathbf{t}^{\mathrm{s}}_{\mathrm{new},i} &= \mathbf{P}_i^{\mathrm{sT}}\mathbf{x}_{\mathrm{new}} \\
\hat{\mathbf{x}}^{\mathrm{s}}_{\mathrm{new},i} &= \mathbf{P}^{\mathrm{s}}_i\mathbf{t}^{\mathrm{s}}_{\mathrm{new},i} = \mathbf{P}^{\mathrm{s}}_i\mathbf{P}_i^{\mathrm{sT}}\mathbf{x}_{\mathrm{new}} \\
\mathbf{e}^{\mathrm{s}}_{\mathrm{new},i} &= \mathbf{x}^{\mathrm{s}}_{\mathrm{new}} - \hat{\mathbf{x}}^{\mathrm{s}}_{\mathrm{new},i} = \left(\mathbf{I} - \mathbf{\Omega}_i\mathbf{\Omega}_i^{\mathrm{T}}\right)\mathbf{x}_{\mathrm{new}}
\end{aligned} \tag{8}$$

Subsequently, the monitoring statistics, T^2 and SPE statistics, are then calculated, respectively, as below

$$\begin{aligned}
T^{\mathrm{c2}}_{\mathrm{new},i} &= \mathbf{b}^{\mathrm{cT}}_{\mathrm{new},i}\mathbf{O}^{-1}_{i,\mathrm{c}}\mathbf{b}^{\mathrm{c}}_{\mathrm{new},i} \\
T^{\mathrm{s2}}_{\mathrm{new},i} &= \mathbf{t}^{\mathrm{sT}}_{\mathrm{new},i}\mathbf{O}^{-1}_{i,s}\mathbf{t}^{\mathrm{s}}_{\mathrm{new},i} \\
\mathrm{SPE}^{\mathrm{s}}_{\mathrm{new},i} &= \mathbf{e}^{\mathrm{sT}}_{\mathrm{new},i}\mathbf{e}^{\mathrm{s}}_{\mathrm{new},i}
\end{aligned} \tag{9}$$

If the patterns behave normally, that is, steady phase status, they should be all well below the confidence limit. Or else, process fault is detected.

2. For the pattern between any two phase centers ($\mathbf{X}_i$ and $\mathbf{X}_j$), where $\mathbf{X}_i$ is the starting phase and $\mathbf{X}_j$ is the target phase, its time location is considered. Generally, when it is near to each phase center, it is more possible that the pattern is in steady phase status, whereas when it is far from the phase center, it is more possible that the pattern is in transition. The corresponding systematic variation and residual are calculated by projecting it onto the starting-phase models as calculated in Eq. 8. If all monitoring statistics stay well within the predefined normal regions in both subspaces, the current operation pattern can be well described by single phase. So the current sample can be deemed to be operating according to the normal operation rule of this phase instead of transition pattern. On the contrary, when out-of-control monitoring alarms are issued, which means that the current phase is not enough to capture the current pattern, the next phase's characteristics are influential or one process fault is occurring. To identify the real cause, the between-phase transition is further analyzed in the following subsection.

Between-phase transition identification

As analyzed before, because of various reasons, especially the uncertainty and diversification of transition operations, it may be difficult to obtain a determinate monitoring model to track dynamic transition patterns comprehensively enough. It thus would be more attractive if dynamic transition processes can be supervised online with no prior modeling. Actually, the close relationships between the transition pattern and its neighboring phases can be explained and reconstructed by the common and specific bases of those neighboring phases. The transition trend will be reflected by the changes in the common scores along the common bases and the switching of the specific-to-phase bases.

Actually, each transition sample covers three types of underlying characteristics, $\mathbf{P}_{i-j,\mathrm{g}}$, $\mathbf{P}^{\mathrm{s}}_{i-j}$, and $\mathbf{P}^{\mathrm{s}}_{j-i}$, which are the common bases and the specific bases in $\mathbf{X}_i$ and $\mathbf{X}_j$, respectively. Therefore, the residual, after the explanation of $\mathbf{\Omega}_{i-j} = [\mathbf{P}_{i-j,\mathrm{g}}, \mathbf{P}^{\mathrm{s}}_{i-j}]$, has two components: the normal noise information and the systematic variation caused by $\mathbf{P}^{\mathrm{s}}_{j-i}$. Then the calculated SPE statistic will go beyond the normal limit when the transition sample is only explained by $\mathbf{\Omega}_{i-j}$ in the same way as shown in Eq. 8. Geometrically, we want to bring $\mathbf{x}_k$ back to the normal region of the start phase (i) along the target phase bases $\mathbf{P}^{\mathrm{s}}_{j-i}$. The reconstructed sample vector ($\mathbf{x}^*_k$) can thus be estimated as follows

$$\mathbf{x}^*_k = \mathbf{x}_k - \mathbf{P}^{\mathrm{s}}_{j-i}\mathbf{t}_{i-j} \tag{10}$$

where $\mathbf{t}_{i-j}$ (subscript $i-j$ means the reconstruction from target phase j in the current starting phase i) is an estimate of the linear combination coefficients, that is, the contribution coefficients of the target phase bases $\mathbf{P}^{\mathrm{s}}_{j-i}$.

It is hoped that the overflowed residual value can be eliminated through the additional explanation of $\mathbf{P}^{\mathrm{s}}_{j-i}$

Table 2. Variation Distribution along PCA Loadings by SubPCA

Phase #	I	II	III	IV
First $\mathbf{P}_c$ (%)	93.94	90.47	71.99	52.99
First two $\mathbf{P}_c$ (%)	97.33	97.36	96.6	89.83

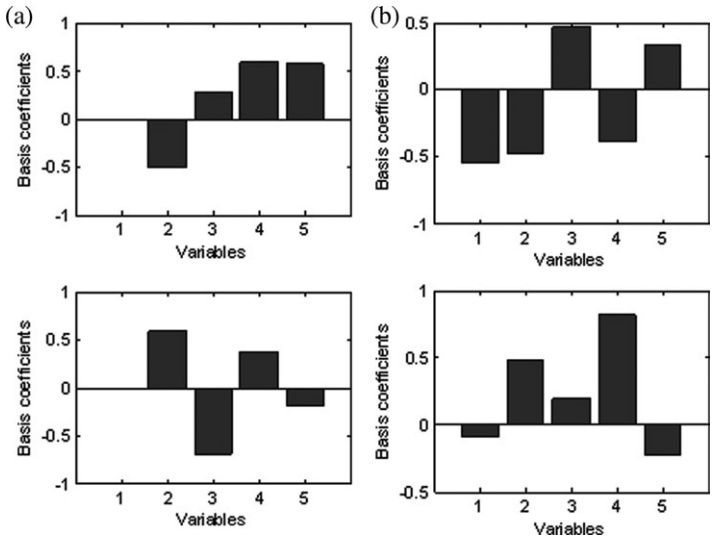

Figure 4. Phase-specific bases for (a) Phase II (top: between Phase Centers I and II; bottom: between Phase Centers II and III) and (b) Phase III (top: between Phase Centers II and III; bottom: between Phase Centers III and IV).

$$
\begin{aligned}
\mathbf{e}_k^{s*} &= \left(\mathbf{I} - \boldsymbol{\Omega}_{i-j}\boldsymbol{\Omega}_{i-j}^{\mathrm{T}}\right)\mathbf{x}_k^* \\
&= \left(\mathbf{I} - \boldsymbol{\Omega}_{i-j}\boldsymbol{\Omega}_{i-j}^{\mathrm{T}}\right)\mathbf{x}_k - \left(\mathbf{I} - \boldsymbol{\Omega}_{i-j}\boldsymbol{\Omega}_{i-j}^{\mathrm{T}}\right)\mathbf{P}_{j-i}^{s}\mathbf{t}_{i-j} \\
&= \mathbf{H}_{\boldsymbol{\Omega}_{i-j}}\mathbf{x}_k - \left(\mathbf{I} - \mathbf{P}_{i-j,\mathrm{g}}\mathbf{P}_{i-j,\mathrm{g}}^{\mathrm{T}} - \mathbf{P}_{i-j}^{s}\mathbf{P}_{i-j}^{s\mathrm{T}}\right)\mathbf{P}_{j-i}^{s}\mathbf{t}_{i-j} \\
&= \mathbf{H}_{\boldsymbol{\Omega}_{i-j}}\mathbf{x}_k - \left(\mathbf{I} - \mathbf{P}_{i-j}^{s}\mathbf{P}_{i-j}^{s\mathrm{T}}\right)\mathbf{P}_{j-i}^{s}\mathbf{t}_{i-j} \\
&= \mathbf{H}_{\boldsymbol{\Omega}_{i-j}}\mathbf{x}_k - \mathbf{H}_{\mathbf{P}_{i-j}^{s}}\mathbf{P}_{j-i}^{s}\mathbf{t}_{i-j} \\
&= \mathbf{H}_{\boldsymbol{\Omega}_{i-j}}\mathbf{x}_k - \boldsymbol{\Pi}_{j-i}\mathbf{t}_{i-j}
\end{aligned}
\tag{11}
$$

where $\mathbf{H}_{\boldsymbol{\Omega}_{i-j}} = \mathbf{I} - \boldsymbol{\Omega}_{i-j}\,\boldsymbol{\Omega}_{i-j}^{\mathrm{T}}$, $\boldsymbol{\Pi}_{j-i} = \mathbf{H}_{\mathbf{P}_{i-j}^{s}}\,\mathbf{P}_{j-i}^{s}$, and $\mathbf{H}_{\mathbf{P}_{i-j}^{s}}$ are the antiprojectors with respect to the column space of $\mathbf{P}_{i-j}^{s}$.

The reconstruction idea is similar to the fault identification algorithm by Dunia and Qin[33] as relative to the start phase, the target phase acts like a process disturbance in the current pattern. As stated in their work, the best estimate of $\mathbf{x}_k^*$ is found by minimizing the SPE monitoring statistic index, $\|\mathbf{e}_k^{s*}\|^2$. Therefore, the reconstruction is given by finding $\mathbf{t}_{i-j}$

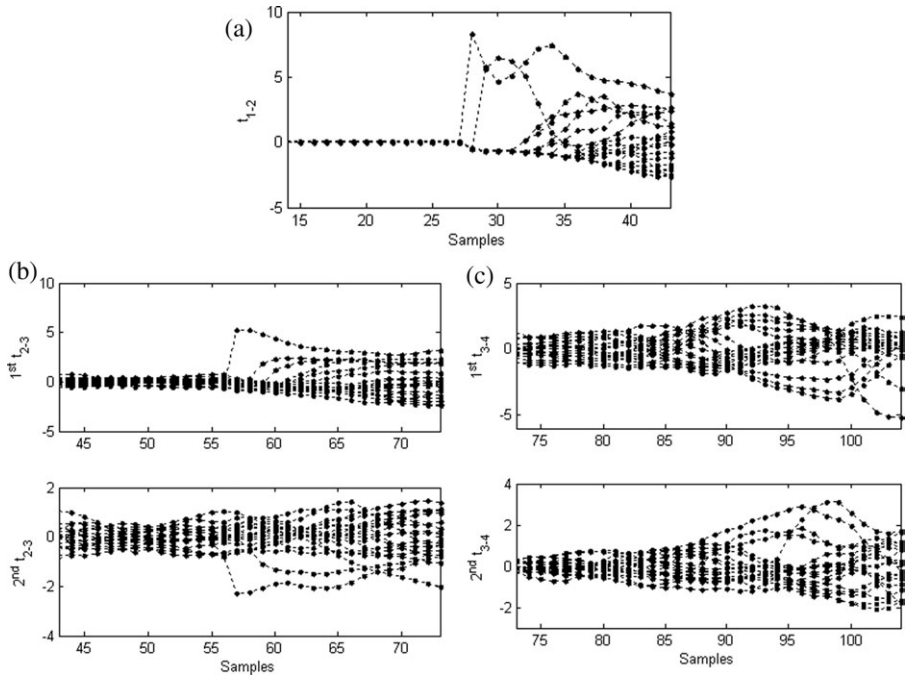

Figure 5. Time-varying trajectory of between-phase reconstruction $\mathbf{t}_{i-j}$ for training data (a) between Phase Centers I and II, (b) between Phase Centers II and III, and (c) between Phase Centers III and IV.

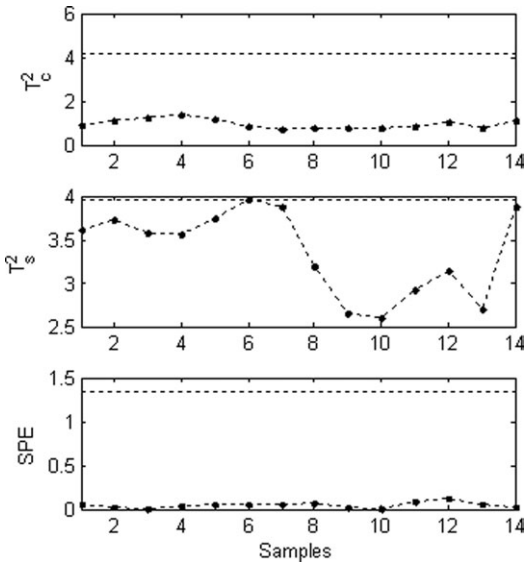

Figure 6. Online monitoring result of a normal batch before Phase Center I (dashed line, 95% control limit; dot line, the monitoring statistics).

$$\begin{aligned}\mathbf{t}_{i-j} &= \arg\min\left\|\mathbf{e}_k^{s*}\right\|^2 = \arg\min\left\|\mathbf{H}_{\mathbf{\Omega}_{i-j}}\mathbf{x}_k - \mathbf{\Pi}_{j-i}\mathbf{t}_{i-j}\right\|^2 \\ &= \left(\mathbf{\Pi}_{j-i}^{\mathrm{T}}\mathbf{\Pi}_{j-i}\right)^{-1}\mathbf{\Pi}_{j-i}^{\mathrm{T}}\mathbf{H}_{\mathbf{\Omega}_{i-j}}\mathbf{x}_k \\ &= \left(\mathbf{P}_{j-i}^{s\mathrm{T}}\mathbf{H}_{\mathbf{P}_{i-j}^s}\mathbf{P}_{j-i}^s\right)^{-1}\mathbf{P}_{j-i}^{s\mathrm{T}}\mathbf{H}_{\mathbf{P}_{i-j}^s}\mathbf{H}_{\mathbf{\Omega}_{i-j}}\mathbf{x}_k\end{aligned} \tag{12}$$

Actually, the reconstruction $\mathbf{t}_{i-j}$ is the weight attached to the target phase model. Generally, when the pattern is nearer to the target phase, $\mathbf{t}_{i-j}$ shows larger magnitude, revealing greater influence of the target phase in the current pattern. Then after a certain time, when the current pattern enters the steady status in target phase, it can be well explained by the target phase. So the residuals after its explanation may not cover any systematic information, and the specific scores in the starting phase may approximate to zero.

So it will be checked whether the original out-of-control information resulting from the disturbances different from the starting phase can be eliminated by the target phase. When the SPE value, SPE_k^{s*}, is returned to the normal region of the starting phase, the current operation pattern is judged to be transition one. In contrast, the real process fault cannot be reconstructed by any two phases as its underlying characteristics and operation pattern are quite different from the target steady phase. In this way, during online monitoring, the normal steady phase patterns, between-phase transition behavior and real faults can be automatically judged and discriminated real time. Figure 2 presents the flow diagram of the proposed between-phase transition monitoring procedure.

Moreover, it should be noted that from Eq. 12, $\mathbf{t}_{i-j}$ can be uniquely calculated if and only if $(\mathbf{\Pi}_{j-i}^{\mathrm{T}}\ \mathbf{\Pi}_{j-i})^{-1}$ exists. In the work by Dunia and Qin,[33] they have derived the necessary and sufficient conditions for complete reconstructability, allowing one to assess the feasibility of reconstruction-based transition identification. In fact, $\mathbf{G}_{\mathbf{P}_j^s} \cap \mathbf{G}_{\mathbf{P}_i^s} = \mathbf{0}$ is the necessary and sufficient condition for the complete reconstructability, justifying the necessity of between-phase analysis. Through the extraction of between-phase common bases, the between-phase overlapping correlations are removed. Then the specific-to-phase bases will be quite different and will focus on the between-phase complementary relationship, thus are more likely to satisfy this condition.

Illustration and Discussion

Process description and data preparation

In this section, a typical MP batch process with between-phase transition, the three-tank system, is used to illustrate the performance of the proposed method. A schematic diagram is shown in Figure 3a. Five process variables, including two float inputs ($F1$ and $F2$) and three liquid levels ($L1$, $L2$, and $L3$) in order, are measured in real time. The operation trajectories of the five measurement variables are illustrated in Figure 3b where standard deviation (STD) index, a widely used measurement of variability or diversity, is used to show how much batch-wise variation or dispersion is there from the average trajectory. Also it can be seen that the magnitude of variability actually varies in different time regions of the process. During the operation process, two

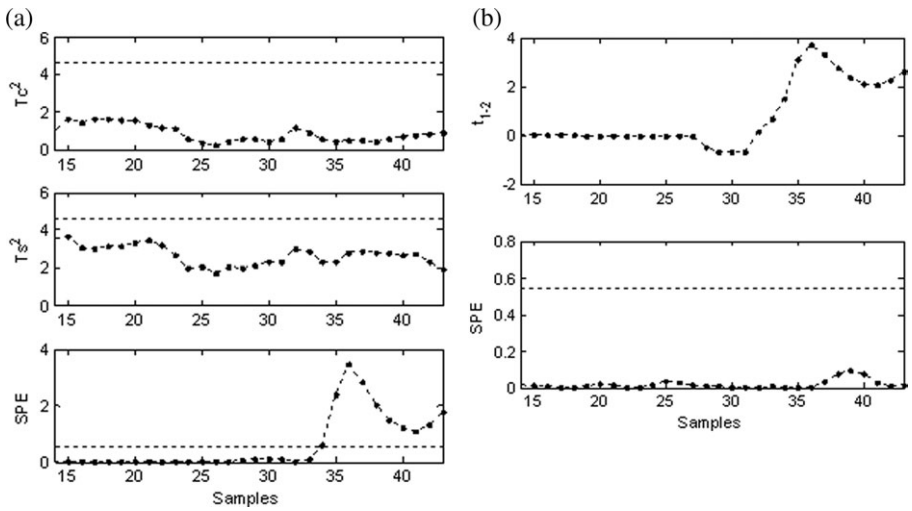

Figure 7. (a) Online monitoring result of a normal batch between Phase Centers I and II and (b) reconstruction-based transition identification result (top: time-varying trajectory of t_{1-2} and bottom: SPE monitoring results) (dashed line, 95% control limit; dot line, the monitoring statistics).

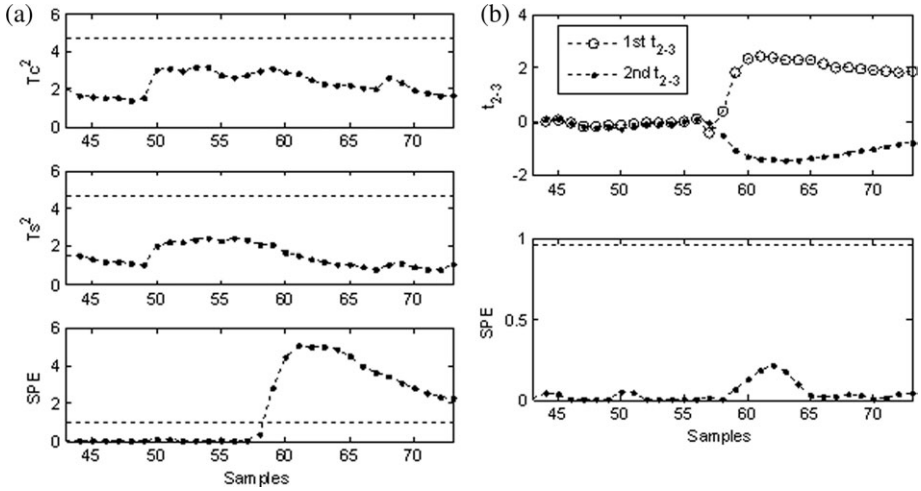

Figure 8. (a) Online monitoring result of a normal batch between Phase Centers II and III and (b) reconstruction-based transition identification result (top: time-varying trajectory of t_{2-3} and bottom: SPE monitoring results) (dashed line, 95% control limit; dot line, the monitoring statistics).

levels, $L1$ and $L2$, are brought from their initial conditions to the set points: $L1 = 300$ mm and $L2 = 200$ mm; whereas $L3$ is left to float to reflect the interaction between Tanks 1 and 2. The rising water levels result in strong process dynamics, and the closed-loop control of liquid levels generates the strong correlations between process variables. The process finishes after the three levels stabilize over a period of time. Nineteen normal experiments, each collecting 120 points of historical data, are carried out under the same conditions, giving a set of modeling samples at different operation statuses.

Simulation result and analysis

The three-tank process is a typical MP batch process with between-phase transition, which can be readily partitioned into four phases using the clustering algorithm,[24] as shown in Figure 3b along with the process variable trajectories, revealing different underlying variable correlations over different phases. Then four phase centers are picked up, which are Samples 14, 43, {72,73}, and {103,104}, respectively, as well as three between-phase possible transition regions ranging between any two neighboring centers.

First, for each phase, between-phase analysis is performed. The common basis extraction results are shown in Tables 1 and 2. The $\mathbf{P}_g$ between Phases I and II reveals that three liquid levels operate similarly in the two phases, which can also be supported by the plot shown in Figure 3b. Clearly, except Phases I and IV, the other phases will be decomposed into two subspaces differently when different adjacent phases are used as their between-phase combination. For example, for Phase II, when it is characterized for analysis between Phases I and II and between Phases II and III, respectively, the common basis extraction results are quite different. Moreover, in each phase, by projecting the measurement data $\mathbf{X}_i$ onto the common bases, the associated variation information along each common base can be obtained. The variations driven by the common bases are quantitatively calculated corresponding to different phase and are also shown in Tables 1 and 2. They are different for different between-phase analyses. From the results, Phase II is explained more (64.03%) by the common basis from between Phases II and III analysis compared with that (only 7.91%) by the common basis from between Phases I and II analysis. After the explanation of common bases in each

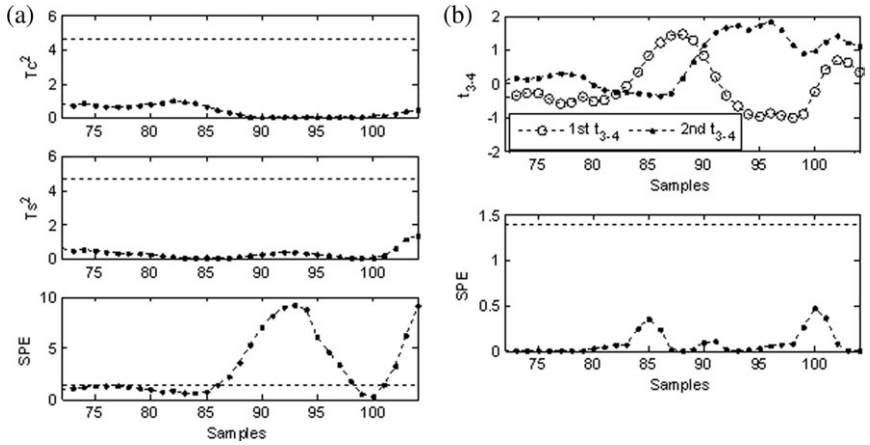

Figure 9. (a) Online monitoring result of a normal batch between Phase Centers III and IV and (b) Reconstruction-based transition identification result (top: time-varying trajectory of t_{3-4} and bottom: SPE monitoring results) (dashed line, 95% control limit; dot line, the monitoring statistics).

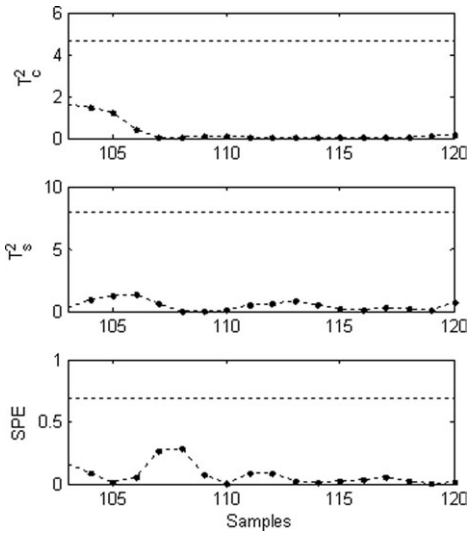

Figure 10. Online monitoring result of a normal batch after Phase Center IV (dashed line, 95% control limit; dot line, the monitoring statistics).

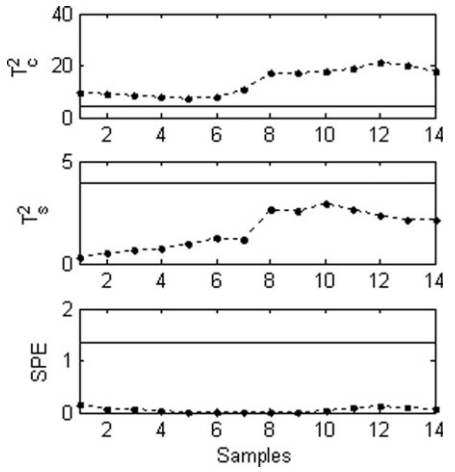

Figure 11. Fault I detection results before Phase Center I (solid line, 99% control limit; dot line, on-line monitoring statistics).

phase, specific bases are extracted to indicate the phase-specific correlations different from its neighboring phases. As shown in Figures 4a, b, for Phase II, when it is analyzed with Phase I as the starting phase, Variable 2 is negatively significant, Variable 3 is not important, and Variables 4 and 5 are both positively important. Comparatively, when Phase II is analyzed with Phase III, Variable 2 is positively significant, Variable 3 is negatively important, and neither Variable 4 nor 5 is dominative with opposite sign. So when each phase is involved for different between-phase analysis, the extracted specific bases may have different dominative variables with different signs. As shown in top plot of Figure 4b, for between Phases II and III, the most dominative variable is $F1$, indicating changes from Phase Center II to III, which agrees well with the trajectory shown in Figure 3b. For between Phases III and IV, as shown in bottom plot of Figure 4b, the most dominative variable is $L2$, whose change is also supported by its trajectory from 72nd to 104th sample shown in Figure 3b. Moreover, it should point out that resulting from the complex coupling relationship among variables, the variables associated with dominative specific basis parameters do not necessarily change greatly between the neighboring phase centers. For example, $F2$, $L1$, and $L3$ in Phase II for between II and III analysis. Also along the first specific basis in each phase, the variations are different. As shown in Tables 1 and 2, for Phase II, variation along common basis is greater in between Phases II and III analysis, whereas variation along specific basis counts more in between Phases I and II analysis. In different between-phase combinations, only one common basis is needed to reveal the between-phase universal information, and one or two specific bases are needed to describe the phase-dependent information. That is, for each phase center, when it is associated with different neighboring phases for between-phase analysis, it is decomposed differently based on its relationship with its neighboring phase. The variation information explained by the first common basis and specific basis in each phase is summed to see how much information can be captured by them. Comparatively, the variation based on subPCA is also calculated to see how the variance distribution is along the first subPCA loading and the first two loadings, respectively. Clearly, the subspace separation results give a different description for each phase from the between-phase viewpoint. Regarding subPCA, we can only know the scenario in each isolated phase but cannot get any idea about its relationships with its neighboring phases. By considering the between-phase relationship, interesting information is revealed to help phase transition analysis.

Table 3. Process Faults Introduced in the Three-Tank System

Fault No.	Fault Description	Occurrence Time
1	A leakage in Tank 1 by fully opening valve LV1	First sample
2	Level sensor failure in Tank 2	40th sample
3	A leakage in Tank 1 by half opening valve LV1	60th sample
4	A leakage of Tanks 2 and 3 by fully opening valves LV2 and LV3 simultaneously	48th sample

Then based on between-phase analysis, different statistical models are designed, revealing the relationship between any two phases, for online monitoring in each phase. First, the irregular transition dynamics are demonstrated by checking the time-varying trajectory of between-phase reconstruction score $\mathbf{t}_{i-j}$ for training data as calculated in Eq. 12. As mentioned before, the reconstruction $\mathbf{t}_{i-j}$ is the weight attached to the target phase model. Its magnitude thus reveals the influence of the target phase during the transition, which is supposed to increase generally. As shown in Figure 5a, right after the Phase Center I (14th sample), $\mathbf{t}_{i-j}$ for all batches are almost zero, which means that the patterns are in steady status within Phase I. After 27th sample, $\mathbf{t}_{i-j}$ of some batches begin to show larger magnitude, whereas others do not until later. Besides the magnitude of $\mathbf{t}_{i-j}$, its signs and changing timings are also different over batches, revealing the irregular transition phenomena. Also it tells that the weights to the target-phase models may be negative. The similar phenomenon can be seen in Figures 5b, c for reconstruction $\mathbf{t}_{i-j}$ along the two specific bases in each target

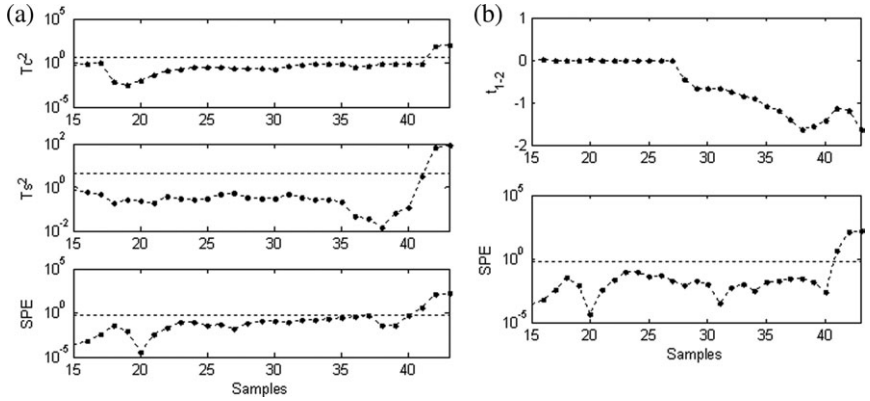

Figure 12. Fault II detection results between Phase Centers I and II (a) monitoring statistics and (b) SPE monitoring statistics after transition reconstruction (solid line, 99% control limit; dot line, on-line monitoring statistics).

phase. Generally, when the pattern is nearer to the target phase, $\mathbf{t}_{i-j}$ shows larger magnitude, revealing greater influence of the target phase in the current pattern. Moreover, the magnitude of $\mathbf{t}_{i-j}$ does not consistently increase along time direction, revealing time-varying transition irregularity. Then after a certain time, when the current pattern enters the steady status in target phase, it can be well explained by the target phase. So the residuals after the explanation of target phase may not cover systematic information, and the specific scores in the starting phase may approximate to zero, which are not shown here.

Then the monitoring systems are tested online. For one normal batch, from the process starting, before the center of Phase I, the three monitoring statistics are shown in Figure 6, which are well below the confidence limit, agreeing with the real case. Then starting from Phase Center I (14th sample) till Phase Center II (43rd sample), the monitoring results are shown in Figure 7a. At the beginning, all monitoring statistics stay well within the normal region, revealing that the patterns are now in steady status of Phase I. Then after the 34th sample, SPE statistics values go beyond the control limit, revealing that the underlying characteristics of the pattern cannot be fully addressed only by Phase I. To check whether the alarm is caused by process failure or phase transition, the reconstruction-based monitoring results are shown in Figure 7b. From the 27th sample, the reconstruction $\mathbf{t}_{1-2}$ begins depart from zero, and shows large increase consistent with that shown in SPE statistics in Figure 7a as the contributions of $\mathbf{P}^{s}_{2-1}$ are becoming more dominating. After the explanation of target phase, the out-of-control SPE values are eliminated, which means that the original deviation from the starting phase is well explained by target phase. Then this is normal transition pattern. Between Phase Centers II and III (from 43rd to 73rd sample), as shown in Figure 8a, the SPE monitoring values escape from the desired operation trajectory from the 60th sample. Similarly, reconstruction results are performed along the two specific bases in target phase center, where the first reconstruction score $\mathbf{t}_{2-3}$ plays more importantly than the second one. The transition is judged correctly as SPE is brought back to its expected region as shown in Figure 8b. Similarly, within the transition region between Phase Centers III and IV, the transition pattern is tracked well as shown in Figure 9. After Phase Center IV (104th sample), the pattern is supposed to be in steady status of Phase IV, which is supported by the monitoring result shown in Figure 10.

Further, four fault types as listed in Table 3 are used to test the fault detection performance, representing different disturbances introduced at different time and into different measurement variables. Based on different between-phase models, the

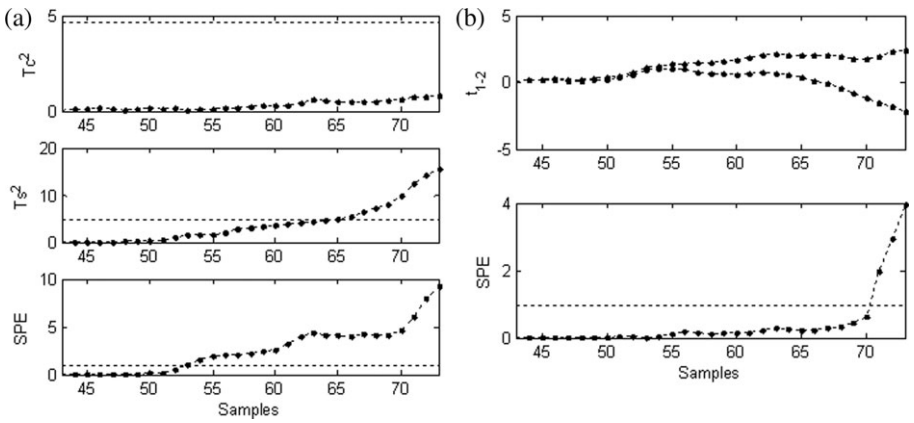

Figure 13. Fault III detection results between Phase Centers II and III (a) monitoring statistics and (b) SPE monitoring statistics after transition reconstruction (solid line, 99% control limit; dot line, on-line monitoring statistics).

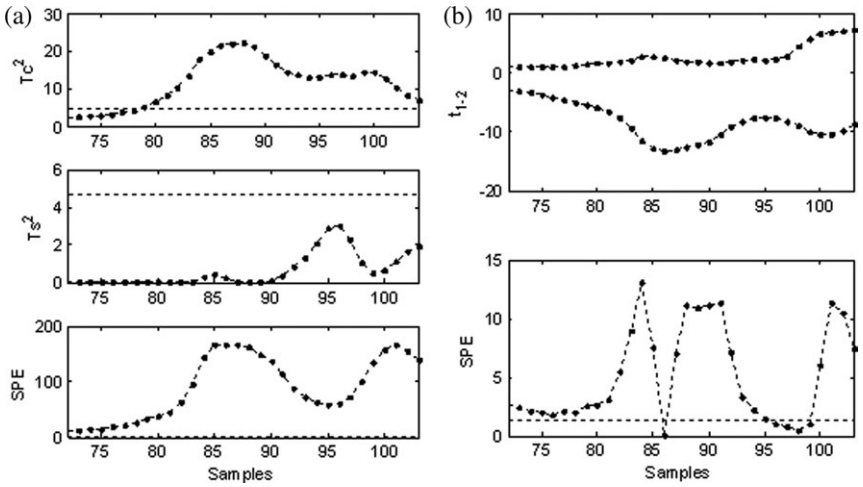

Figure 14. Fault III detection results between Phase Centers III and IV (a) monitoring statistics and (b) SPE monitoring statistics after transition reconstruction (solid line, 99% control limit; dot line, on-line monitoring statistics).

monitoring results for the four faults are shown in Figures 11–15, respectively. For all cases, in general, none of them can remove the disturbed variation and bring the SPE monitoring statistics back to the normal region, which means that all the faults are clearly detected. Specially, for Fault I that happens at the right beginning of the process, the monitoring is conducted based on Phase I model, where the T^2-statistic based on common bases go out of normal region from the first sample as shown in Figure 11, revealing abnormal disturbances. In Figure 12a, for Fault II occurring at 40th sample (between Phase Centers I and II), all monitoring statistics almost yield alarm signals right after the occurrence of sensor failure. Further using reconstruction-based transition identification, SPE alarms cannot be removed as shown in Figure 12b, revealing that the alarms result from a process fault instead of a normal between-phase transition. The monitoring results for Fault III (introduced at 60th sample, between Phase Centers II and III) are shown in Figure 13a. The T^2-statistic based on specific bases goes out of normal region after 60th sample and SPE-statistic before 60th sample. Then using reconstruction-based transition identification, SPE alarms before 60th sample are removed as shown in Figure 13b, revealing that those alarms might result from the between-phase transition instead of process failure. Also, the SPE alarms between 60th and 70th samples are eliminated, showing a certain time delay for fault detection, which may result from the smaller fault influence compared with Fault I. In addition, in Figure 13b, as the SPE monitoring statistics after reconstruction show out-of-control alarms near Phase Center III, for comparison, the monitoring results between Phase Centers III and IV are shown in Figure 14 with respect to the same fault, where by Phase III model, the SPE monitoring statistics

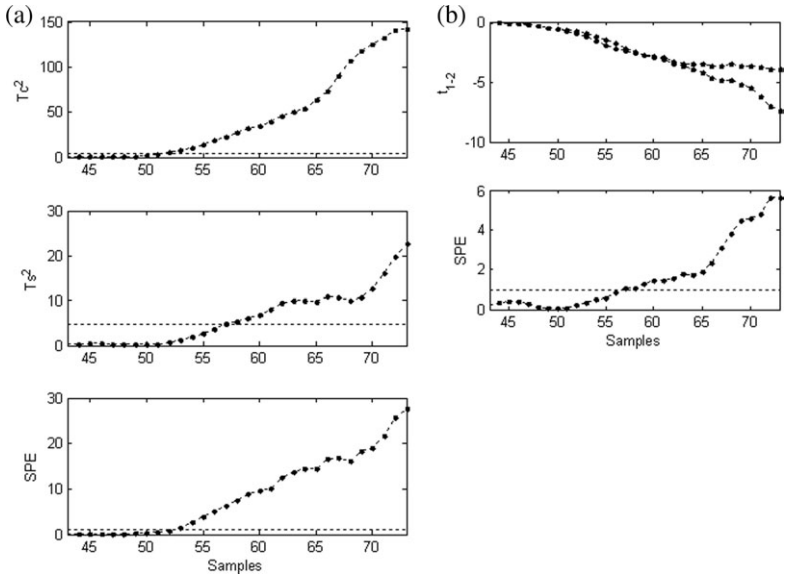

Figure 15. Fault IV detection results between Phase Centers II and III (a) monitoring statistics and (b) SPE monitoring statistics after transition reconstruction (solid line, 99% control limit; dot line, on-line monitoring statistics).

clearly indicate the abnormality and out-of-control alarms cannot be eliminated by reconstruction. Also the results reveal that the influence of Fault III is continuously forward in the process. For Fault IV at 48th sample (between Phases II and III), all monitoring statistics yield alarm signals but with different delays in Figure 15a. Then after reconstruction, SPE alarms cannot be removed, revealing that those alarms result from some process failure instead of the between-phase transition. Also it should be noted that after transition reconstruction, the alarm time (57th sample) by the SPE plot in Figure 15b shows larger delay than before (53rd sample) in Figure 15a.

With the proposed method, the ideas of between-phase similarity and dissimilarity are better understood. By relating the correlations between the underlying variables of two neighboring phases and separating their common and unique information, the proposed method can provide a better characterization of each phase. The changes from one phase to another are thus better tracked, beneficial for between-phase transition analysis and monitoring. There may still be many issues to be investigated in the future, but the results of this study provide the basis for further work and improvement. For example, it may lead to improved knowledge regarding critical variables that dominate phase changeovers, increasing the possibilities of and the potential for active phase-based process control.

Conclusions

This article proposes a process analysis, understanding, and monitoring methodology for between-phase transition in MP batch processes. It first reveals the problem of irregular transition dynamics over batches. Instead of identifying the definite boundary between steady phase and transition and fixing transition model a priori, only phase centers are defined, between any two of which, all process patterns are regarded as possible transitions to accommodate their irregular dynamics. By between-phase modeling, the underlying phase information is decomposed more meaningfully for between-phase transition analysis. The strengths of the proposed strategy lie not only in the effectiveness of the monitoring methodology but also in the appealing analysis results and comprehension for between-phase transition problem. Different from the conventional modeling strategy, the proposed method reduces the efforts of model development for between-phase transitions. Instead, the dynamic transition patterns are automatically monitored by means of two neighboring-phase models and the reconstruction calculation, which is simple and not computationally demanding. The Illustration to a practical experimental system illustrates the existence of ''irregular transition'' phenomena and the effectiveness of the proposed analysis strategy. Moreover, further analyses can also be conducted focusing on the robustness of the proposed method, which needs further demonstration based on more real cases under different practical environments. It also provides the basis and potential for future work. For example, the proposed method may be proper for continuous processes to address the mode transition problem, which, however, needs further and specific consideration regarding their different characteristics from batch processes.

Acknowledgments

This work is supported in part by the China National 973 program (2009CB320603) and RGC-NSFC joint project under project number N_HKUST639/09.

Literature Cited

1. Nomikos P, MacGregor JF. Monitoring batch processes using multiway principal component analysis. *AIChE J*. 1994;40:1361–1375.
2. Nomikos P, MacGregor JF. Multivariate SPC charts for monitoring batch processes. *Technometrics*. 1995;37:41–59.
3. Nomikos P, MacGregor JF. Multi-way partial least squares in monitoring batch processes. *Chemom Intell Lab Syst*. 1995;30:97–108.
4. Kosanovich KA, Dahl KS, Piovoso MJ. Improved process understanding using multiway principal component analysis. *Ind Eng Chem Res*. 1996;35:138–146.
5. Westerhuis JA, Kourti T, MacGregor JF. Comparing alternative approaches for multivariate statistical analysis of batch process data. *J Chemom*. 1999;13:397–413.
6. Wise BM, Gallagher NB, Butler SW, White DD, Barna GG. A comparison of principal component analysis, multiway principal component analysis, trilinear decomposition and parallel factor analysis for fault detection in a semiconductor etch process. *J Chemom*. 1999;13:379–396.
7. van Sprang ENM, Ramaker H-J, Westerhuis JA, Gurden SP, Smilde AK. Critical evaluation of approaches for on-line batch process monitoring. *Chem Eng Sci*. 2002;57:3979–3991.
8. Undey C, Cinar A. Statistical monitoring of multistage, multiphase batch processes. *IEEE Control Syst Mag*. 2002;22:40–52.
9. Chen J, Liu K-C. On-line batch process monitoring using dynamic PCA and dynamic PLS models. *Chem Eng Sci*. 2002;57:63–75.
10. Undey C, Ertunc S, Cinar A. Online batch/fed-batch process performance monitoring, quality prediction, and variable-contribution analysis for diagnosis. *Ind Eng Chem Res*. 2003;42:4645–4658.
11. Albazzaz H, Wang XZ. Statistical process control charts for batch operations based on independent component analysis. *Ind Eng Chem Res*. 2004;43:6731–6741.
12. Yu J, Qin SJ. Multiway Gaussian mixture model based multiphase batch process monitoring. *Ind Eng Chem Res*. 2009;48:8585–8594.
13. Zhao C, Gao F, Wang F. Phase-based joint modeling and spectroscopy analysis for batch processes monitoring. *Ind Eng Chem Res*. 2009;49:669–681.
14. Kosanovich KA, Piovoso MJ, Dahl KS, MacGregor JF, Nomikos P, *Multi-way PCA applied to an industrial batch process*. In: *Proceedings of the American Control Conference*, Baltimore, MD. 1994:1294–1298.
15. Dong D, McAvoy TJ, *Multi-stage batch process monitoring*. In: *Proceedings of the American Control Conference*, Seattle, WA, 1995:1857–1861.
16. Kourti T, Nomikos P, MacGregor JF. Analysis, monitoring and fault diagnosis of batch processes using multiblock and multiway PLS. *J Process Control*. 1995;5:277–284.
17. Lu N, Gao F, Wang F. Sub-PCA modeling and on-line monitoring strategy for batch processes. *AIChE J*. 2004;50:255–259.
18. Camacho J, Pic J. Online monitoring of batch processes using multiphase principal component analysis. *J Process Control*. 2006;16:1021–1035.
19. Camacho J, Pic J. Multi-phase principal component analysis for batch processes modelling. *Chemom Intell Lab Syst*. 2006;81:127–136.
20. Doan XT, Srinivasan R, Bapat PM, Wangikar PP. Detection of phase shifts in batch fermentation via statistical analysis of the online measurements: a case study with rifamycin B fermentation. *J Biotechnol*. 2007;132:156–166.
21. Liu J, Wong DSH. Fault detection and classification for a two-stage batch process. *J Chemom*. 2008;22:385–398.
22. Maiti SK, Srivastava RK, Bhushan M, Wangikar PP. Real time phase detection based online monitoring of batch fermentation processes. *Process Biochem*. 2009;44:799–811.
23. Zhao C, Wang F, Mao Z, Lu N, Jia M. Adaptive monitoring based on independent component analysis for multiphase batch processes with limited modeling data. *Ind Eng Chem Res*. 2008;47:3104–3113.
24. Lu N, Gao F, Yang Y, Wang F. PCA-based modeling and on-line monitoring strategy for uneven-length batch processes. *Ind Eng Chem Res*. 2004;43:3343–3352.
25. Yao Y, Gao F. A survey on multistage/multiphase statistical modeling methods for batch processes. *Annu Rev Control*. 2009;33:172–183.
26. Zhao C, Wang F, Lu N, Jia M. Stage-based soft-transition multiple PCA modeling and on-line monitoring strategy for batch processes. *J Process Control*. 2007;17:728–741.
27. Yao Y, Gao F. Phase and transition based batch process modeling and online monitoring. *J Process Control*. 2009;19:816–826.

28. Zhao C, Gao F, Niu D, Wang F. A two-step basis vector extraction strategy for multiset variable correlation analysis. *Chemom Intell Lab Syst*. 2011;107:147–154.
29. Lowry CA, Montgomery DC. A review of multivariate control charts. *IIE Trans*. 1995;27:800–810.
30. Ryan TP. *Statistical Methods for Quality Improvement*. New York: Wiley, 1989.
31. Box GEP. Some theorems on quadratic forms applied in the study of analysis of variance problems, I. Effect of inequality of variance in the one-way classification. *Ann Math Stat*. 1954;25:290–302.
32. Jackson JE, Mudholkar GS. Control procedures for residuals associated with principal component analysis. *Technometrics*. 1979;21:341–349.
33. Dunia R, Qin SJ. Subspace approach to multidimensional fault identification and reconstruction. *AIChE J*. 1998;44:1813–1831.
34. Carroll JD. *Generalization of canonical correlation analysis to three or more sets of variables*. In: *Proceeding of the 76th convention of the American Psychological Association*, San Francisco, CA. Vol. 3, 1968:227–228.

Appendix

In the case of multiset measurement data, $\mathbf{X}^i$ ($N_i \times J$) ($i = 1,2,\ldots C$), the set-to-set interrelation may refer to the common structures in variable correlations. In each measurement space, it is always possible to find out a subset of samples, which are representative enough to the other samples and can substitute all samples by their linear combinations. The major underlying variable correlations in the original measurement space are also represented by them. They are called subbasis vectors here, which are used to evaluate the similarity and dissimilarity over multiple sets.

As any subbasis in each dataset space, $\mathbf{p}_j^i$ ($j = 1,2,\ldots,J$), must lie in the span of the input observations, there exists linear combination coefficients $\mathbf{a}_j^i = [a_{1,j}^i, a_{2,j}^i,\ldots,a_{n,j}^i]$, such that

$$\mathbf{p}_j^i = \sum_{n=1}^{N_i} a_{n,j}^i \mathbf{x}_n^i = \mathbf{X}^{i\mathrm{T}} \mathbf{a}_j^i \tag{A1}$$

That is, each subbasis vector $\mathbf{p}_j^i$ is actually a linear function of the original observations in each dataset.

The degree of similarity of subbasis vectors should be measured in terms of "how close with each other over sets." However, it would be complicated if all set-to-set interrelationships are simultaneously and directly evaluated. Here, the computation trick by Carroll[34] is borrowed, in which, a third-party canonical variate was introduced in their generalized component analysis (GCA) algorithm. Then in our method, the simultaneous similarity assessment of variable correlations over sets can be achieved through the introduction of a global and common basis vector, $\mathbf{p}_\mathrm{g}$. It can be regarded as the supplementary and pseudo ($C + 1$)st subbasis vector and should approximate all C subbases as close as possible. That is, these real subbasis vectors, which are correlated with each other as close as possible, or speaking more exactly, as common as possible over sets, can be comprehensively described and even substituted by the global basis.

To figure out the common bases, a two-step extraction procedure is designed. In the first step, the common subbases are preparatorily computed from the original measurement data, and then in the second step they can be further condensed and refined by enhancing their correlations. Different optimization objectives and constraints are used in the two steps, which both come down to the simple analytic solutions of constrained optimization problems.

The first-step basis extraction

During the first-step basis extraction, we define it in terms of finding a J-dimensional global basis ($\mathbf{p}_\mathrm{g}$) together with different linear combinations of the observations comprising each of C collective data sets with the cost function and certain constraints as below

$$\max R^2 = \max \sum_{i=1}^{C} \left(\mathbf{p}_\mathrm{g}^\mathrm{T} \mathbf{X}^{i^\mathrm{T}} \mathbf{a}^i\right)^2 \quad s.t. \begin{cases} \mathbf{p}_\mathrm{g}^\mathrm{T} \mathbf{p}_\mathrm{g} = 1 \\ \mathbf{a}^{i\mathrm{T}} \mathbf{a}^i = 1 \end{cases} \tag{A2}$$

Using a Lagrange operator, the optimization problem finally leads to a simple analytic solution

$$\sum_{i=1}^{C} \left(\mathbf{X}^{i\mathrm{T}} \mathbf{X}^i\right) \mathbf{p}_\mathrm{g} = \lambda_\mathrm{g} \mathbf{p}_\mathrm{g} \quad \mathbf{Q}\mathbf{p}_\mathrm{g} = \lambda_\mathrm{g} \mathbf{p}_\mathrm{g} \tag{A3}$$

This is a standard algebra problem. At the request of the maximal objective function value, that is, the largest λ_g, analytically, the solution leads to the eigenvalue decomposition on the sum of subset covariances, $\mathbf{Q} = \sum_{i=1}^{C} \left(\mathbf{X}^{i\mathrm{T}} \mathbf{X}^i\right)$.

The subbasis vector is calculated by

$$\mathbf{p}_i = \mathbf{X}^{i\mathrm{T}} \mathbf{a}^i = \sqrt{\frac{1}{\lambda_i}} \mathbf{X}^{i\mathrm{T}} \mathbf{X}^i \mathbf{p}_\mathrm{g} \tag{A4}$$

where the parameter λ_i can be calculated by $\mathbf{p}_\mathrm{g}^\mathrm{T}\ \mathbf{X}^{i\mathrm{T}}\ \mathbf{X}^i\ \mathbf{p}_\mathrm{g} = \lambda_i$.

Orderly, $\overline{R}$ number of global basis vectors can be derived by Eq. A3 in accordance with the descending λ_g, resulting in the same number of subbasis vectors calculated using Eq. A4 in each dataset. This decomposition summarizes and compresses the underlying cross-set common variable correlations into a new subspace spanned by $\overline{R}$ subbases within each dataset, $\overline{\mathbf{P}}^i$ ($\overline{R} \times J$).

The second-step basis extraction

To get the cross-set common subbases that are really close correlated, correlation analysis index should be used instead of the covariance index. In comparison with the optimization function and constraints shown in Eq. A2, the second-step basis extraction is designed by constructing and solving a different optimization problem. It is implemented on the basis of the first-step analysis result ($\overline{\mathbf{P}}^i$ ($\overline{R} \times J$)), and the aim is to maximize the mean square correlations

$$\max R^2 = \max \sum_{i=1}^{C} r^2\left(\mathbf{p}_\mathrm{g}, \mathbf{P}^{i\mathrm{T}} \mathbf{a}^i\right) = \max \sum_{i=1}^{C} \left(\mathbf{p}_\mathrm{g}^\mathrm{T} \mathbf{P}^{i\mathrm{T}} \mathbf{a}^i\right)^2 \quad s.t. \begin{cases} \mathbf{p}_\mathrm{g}^\mathrm{T} \mathbf{p}_\mathrm{g} = 1 \\ \mathbf{a}^{i\mathrm{T}} \overline{\mathbf{P}}^i \overline{\mathbf{P}}^{i\mathrm{T}} \mathbf{a}^i = 1 \end{cases} \tag{A5}$$

Using a Lagrange operator, its solution also comes down to a standard algebra problem

$$\sum_{i=1}^{C}\left(\bar{\mathbf{P}}^{i\mathrm{T}}\left(\bar{\mathbf{P}}^{i}\bar{\mathbf{P}}^{i\mathrm{T}}\right)^{-1}\bar{\mathbf{P}}^{i}\right)\mathbf{p}_{\mathrm{g}}=\lambda_{\mathrm{g}}\mathbf{p}_{\mathrm{g}}$$
$$\mathbf{S}\mathbf{p}_{\mathrm{g}}=\lambda_{\mathrm{g}}\mathbf{p}_{\mathrm{g}} \tag{A6}$$

Therefore, the optimization problem finally leads to a simple analytical solution, that is, $\mathbf{p}_{\mathrm{g}}$ should be the eigenvector of $\mathbf{S}=\sum_{i=1}^{C}\left(\bar{\mathbf{P}}^{i\mathrm{T}}\left(\bar{\mathbf{P}}^{i}\bar{\mathbf{P}}^{i\mathrm{T}}\right)^{-1}\bar{\mathbf{P}}^{i}\right)$ corresponding to the largest eigenvalue λ_{g}.

The subbasis vector is calculated by

$$\mathbf{p}_{i}=\bar{\mathbf{P}}^{i\mathrm{T}}\mathbf{a}^{i}=\frac{1}{\sqrt{\lambda_{i}}}\bar{\mathbf{P}}^{i\mathrm{T}}\left(\bar{\mathbf{P}}^{i}\bar{\mathbf{P}}^{i\mathrm{T}}\right)^{-1}\bar{\mathbf{P}}^{i}\mathbf{p}_{\mathrm{g}} \tag{A7}$$

where the suboptimal objective parameter λ_i can be calculated by $\mathbf{p}_{\mathrm{g}}^{\mathrm{T}}\bar{\mathbf{P}}^{i\mathrm{T}}\ (\bar{\mathbf{P}}^{i}\ \bar{\mathbf{P}}^{i\mathrm{T}})^{-1}\ \bar{\mathbf{P}}^{i}\ \mathbf{p}_{\mathrm{g}}=\lambda_{i}$

In turn, R number of global basis vectors are retained and can construct a global basis subspace $\mathbf{P}_{\mathrm{g}}$ ($R \times J$). Correspondingly, C subbasis subspaces, $\mathbf{P}^{i}$ ($R \times J$), are also derived, which are actually the projected ones from $\mathbf{P}_{\mathrm{g}}$ ($R \times J$) onto $\bar{\mathbf{P}}^{i\mathrm{T}}$.

Manuscript received Jun. 1, 2011, and revision received Sept. 19, 2011.